Structural Basis for Mechanical Anisotropy in Polymorphs of Caffeine-Glutaric Acid Cocrystal

Manish Kumar Mishra,[*,a] Kamini Mishra,[b] Aditya Narayan,[c] C. Malla Reddy*[*,d] and Venu R. Vangala*[*,c]*

[a] Department of Pharmaceutics, College of Pharmacy, University of Minnesota, Minneapolis, MN 55455, USA

[b] Department of Chemistry, School of Advanced Sciences (SAS), VIT University, Vellore-632014, Tamil Nadu, India

[c] Centre for Pharmaceutical Engineering Science and School of Pharmacy and Medical Sciences, University of Bradford, Bradford BD7 1DP, UK

[d] Department of Chemical Sciences, Indian Institute of Science Education and Research (IISER) Kolkata, Mohanpur Campus, Mohanpur 741 246, India

ABSTRACT:

Insights into structure–mechanical property correlations in molecular and multicomponent crystals have recently attracted significant attention owing to their practical applications in the pharmaceutical and specialty fine chemicals manufacturing. In this contribution, we systematically examine the mechanical properties of dimorphic forms, Forms I and II of 1:1 caffeine-glutaric acid cocrystal on multiple faces using nanoindentation to fully understand their mechanical anisotropy and mechanical stability under applied load. Higher hardness, H, and elastic modulus, E, of stable Form II has been rationalized based on its corrugated layers, higher interlayer energy, lower interlayer separation, and presence of more intermolecular interactions in the crystal structure compared to metastable Form I. Our results show that mechanical anisotropy in both polymorphs arises due to the difference in orientation of the same 2D structural features, namely the number of possible slip systems, and strength of the intermolecular interactions with respect to the indentation direction. The mechanical properties results suggest that 1:1 caffeine-glutaric acid cocrystal, metastable form (Form I) could be a suitable candidate with desired tablet performance to that of stable Form II. The overall, it demonstrates that the multiple faces of nanoindentation is critical to determine mechanical

anisotropy and structure- mechanical property correlation. Further, the structural-mechanical property correlations aids in the selection of the best solid phase for macroscopic pharmaceutical formulation.

Pharmaceutical cocrystals are multicomponent crystals that combine an active pharmaceutical ingredient (API) with a suitable pharmaceutical or non-pharmaceutical coformer through crystal engineering, which positively modify the physicochemical properties such as physical and photochemical stability, hygroscopicity, melting point, colour, solubility, dissolution rate, permeability, bioavailability, and mechanical properties.[1-19] The mechanical properties of molecular crystals depend on the molecular arrangement, strength of intermolecular interactions, size and shape of molecules.[11-20] Investigation of structure–mechanical property correlations in molecular crystals has recently drawn a significant attention of researchers due to their potential applications in mechanical processing of pharmaceutical drugs, designing of mechanical actuators, flexible optoelectronic materials, micro-robots, mechanochromic luminescent materials, and mechanical sensors.[21-28] Such investigations propel the determination and prediction of mechanical properties of molecular crystals based on the qualitative deformation like bending behaviors,[13,16] quantitative measurements per se nanoindentation,[14-21] high-pressure powder compaction,[22] spectroscopy,[29,30] and computational methods.[31] In the context of industrial-scale pharmaceutical manufacturing, an understanding of structure–mechanical property relationships can also be used to deliberately alter mechanical properties such as millability and tabletability towards optimal drug development and production. [22,32-34] For instance, a soft solid drug can become a paste during milling, which is undesirable during the production stage of APIs. Stress-induced polymorphic transformations of pharmaceutical crystals is a common phenomenon that occurs during secondary unit processes such as milling, granulation, tableting, etc.[30,35,36] Such phase behaviors can severely affect the manufacturing of APIs as the most stable form of an API is preferably marketed. The structural rearrangement associated with phase transformation during mechanical loading remains poorly understood.

Modern nanoindentation has been successfully employed to study the mechanical properties of a wide range of molecular crystals that are available only in small sizes, with emphasis on crystal structure–property relationships.[13-16,21,30,32] The fundamental understanding

of molecular-level properties such as intermolecular interaction characteristics, crystal packing,[14-16,21] domain coexistence,[30,35,37] layer migration,[38-40] desolvation,[41-42] mechanoluminescence,[43] and solid-state reactivity[15,16] on mechanical properties such as stiffness and strength can be explored through nanoindentation. Mechanical anisotropy, directional dependent physical property of materials, is a critical consideration for materials selection in engineering applications.[14,42,44-46] Nanoindentation can also be used to probe crystal anisotropy, which provides new perspectives on supramolecular bonding that is intrinsic to the crystalline materials.[14-16,42,46] Polymorphism influences the mechanical properties, which offers the opportunities to correlate the structure vs mechanical properties.[13,15,16,21] The variations in mechanical properties of polymorphs of drugs such as aspirin, paracetamol, felodipine, omeprazole, curcumin, and sulfathiazole have been effectively examined using nanoindentation.[12,30,35,37,47-51]

Trask *et al*. have discovered the two polymorphic forms, Forms I and II, of 1:1 caffeine-glutaric acid (CA-GA) cocrystal.[52] The stability of these polymorphs were examined in various studies under different relative humidity (RH) conditions.[53-55] Metastable Form I transforms to thermodynamic Form II within 24 hours and Form II remains stable at ambient conditions for several weeks (stable at 25 °C, 75% RH for at least 7 weeks), however, under high humidity conditions (stable at 25 °C, 98% RH for only 3 days), it transforms to caffeine hydrate.[55] We previously performed *in situ* X-ray diffraction studies on this dimorphic system and determined the thermodynamic relationship of these dimorphs.[54] Thakuria *et al.* utilized *in situ* atomic force microscopy (AFM) and nanoindentation to distinguish these dimorphs and monitored the surface rearrangements of Forms I and II under high humidity conditions.[55,56] Recently, we have demonstrated that planetary ball mill stresses could induce polymorphic transformation from the stable Form II to the metastable Form I due to the local heating effect.[53] Hence, this polymorphic co-crystal has been a good model system for understanding various solid-state aspects of pharmaceutical compounds. However, the structural origins associated with stress-induced phase transformations, which proceed via a slip mechanism, remains unclear for the dimorphs. Accordingly, the main focus of this contribution is to systematically investigate the mechanical properties on multiple faces of dimorphic forms, Forms I and II, of CA−GA cocrystal using nanoindentation to comprehensively understand their mechanical anisotropy and to correlate

them with the underlying structural features vs tablet performance of the dimorphs of CA-GA cocrystal.

Scheme 1. **Molecular Structure of Caffeine and Glutaric acid**

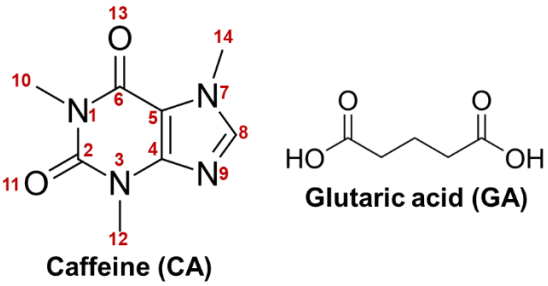

EXPERIMENTAL METHODS

Materials. Anhydrous caffeine (99% purity) from Fluka and glutaric acid (99%) from Alfa-Aesar were obtained and used as received. The solvents were of either analytical or chromatographic grade.

Cocrystal Polymorphs Preparation. Quality single crystals of Forms I and II of CA−GA co-crystal in different morphologies were grown by slow evaporation of a saturated solution containing 1:1 mixture of caffeine and glutaric acid in the following listed solvents at room temperature.

Polymorph	Solvent	Morphology
Form I	Chloroform	Needle
Form II	1:1 mixture of ethyl acetate-chloroform	Block

Single Crystal X-ray Diffraction (SCXRD). Good quality single crystals of CA−GA cocrystal polymorphs were carefully chosen after viewing them under an Olympus microscope supported by rotatable polarizing stage. Single crystal X-ray diffraction data for Form I were collected at room temperature on a Rigaku Mercury 375R/M CCD (XtaLABmini) diffractometer using graphite monochromated Mo-Kα radiation, equipped with a Rigaku low temperature gas spray cooler (see Supporting Information, hereafter referred to as SI, Table S1). The Rigaku crystal

clear software was used to process the data.[57] The structure solution was performed by direct methods, and refinements were performed using SHELX97[58] and WinGX suite[59]. The hydrogen atoms were either placed geometrically from the difference Fourier map or allowed to ride on their parent atoms in the refinement cycles. All non-hydrogen atoms were refined with anisotropic displacement parameters. The carbon atoms of glutaric acid and caffeine of Form I in the asymmetric unit were disordered over two positions related by mirror symmetry with site occupancy values of 0.5. The disorder was refined using Part 1 and Part 2 instructions. The site occupancy factors (SOFs) for both parts were adjusted were approximately equal (50:50), and then they were fixed at those values (details of the disorder refinement strategy are available as part of the deposited crystallographic information file, CCDC 2011984). The crystals of Form II were confirmed with the unit cell parameters collected at room temperature (see SI, Table S1) and compared with the reported polymorphs in the CSD.[53] Face indexing of good quality single crystals for both forms was performed at room temperature on a Rigaku Mercury 375R/M CCD (XtaLABmini) diffractometer with CrystalClear software, and the crystal faces were assigned.

Molecular Electrostatic Potential (MEP) and HOMO-LUMO Calculations. The energy, HOMO-LUMO molecular orbital diagram, electron density, molecular electrostatic potential maps, single point energies and optimized electronic structure of Forms I and II of CA-GA cocrystal at room temperature were computed via density functional theory (DFT) using standard B3LYP functional and 6-311+G(d,p) basis-set calculations at default temperature conditions (298.15 K), as implemented in GAUSSIAN09 (see SI, Figure S1).[60] Pictorial diagrams of molecular geometries were prepared with the program GaussView. Chemcraft was used to obtain atomic coordinates for both the polymorphs. Three-dimensional electrostatic surface potential maps were calculated around the molecule with electron density 0.002 electron/Å. Colour coding was applied to locate negatively charged (red) and positively charged (blue) surfaces.

Nanoindentation Measurements. Large (~1.0×0.5 mm^2 in cross-section and 0.30 mm in thickness), well-shaped, and good quality dried single crystals of CA-GA cocrystal polymorphs were selected through an optical microscope supported by a rotatable polarizing stage for nanoindentation experiments.[61] We have confirmed using optical polarising microscope and high intensity diffraction patterns in the SCXRD that there are no solvent occlusions and intergrown domain defects in the crystals.[61] The crystals were initially washed with paraffin oil to remove

any small crystals that might have been attached to the surface during crystallization. Further, each crystal of CA-GA Form I or II was firmly mounted on a metallic stud using a thin layer of cyanoacrylate glue. Nanoindentation experiments were performed on the two faces, namely (001) and (100), for both polymorphs using the TI Premier Triboindenter from Hysitron, Minneapolis, USA, equipped with an *in-situ* AFM imaging capability. A three-sided pyramidal Berkovich diamond indenter with a tip radius of ~100 nm was used. During nanoindentation, the loading and unloading rates were 0.6 mN/s and the hold time at the peak load of 6 mN was 30 s. Around four to five crystals of each polymorph were examined and a minimum of 20 indentations were performed on each crystal to obtain consistent and reliable average data. For visualization of surface topology, AFM-scanned image with 20 μm×20 μm area containing the indentation mark (see SI, Figure S3) was used. The *P-h* curves obtained were examined using the standard Oliver-Pharr (O-P) method[62] to calculate elastic modulus (*E*) and hardness (*H)* on the indented faces. However, the estimation of *H* using the O-P method would be inaccurate if there is a significant pile-up of material against the indenter.[63] The *H* can be overestimated by up to 60 % and *E* by up to 16 % depending on the extent of pile-up.[63] If *h*f/*h*max < 0.7, pile-up is not a significant factor but the O–P data analysis expected to provide reliable results. Here, *h*f is the final displacement after complete unloading and *h*max is the maximum depth of penetration. The *h*f/*h*max value for both the faces of Form II are less than 0.7, therefore, the *E* and *H* values are not significantly overestimated. However, to obtain the more accurate values of *H* on both faces of Form II, the maximum indentation load, *P*max, divided by the contact area, *A* (it was estimated from AFM- images of the indentation impressions) has been employed.[14,15,35]

Hirshfeld Surface Analysis and Energy Framework calculations. The Hirshfeld surfaces, 2D fingerprint plots, and energy frameworks calculations for intermolecular interaction topologies of CA-GA polymorphs were performed using Crystal-Explorer V.17[64] based on Gaussian B3LYP-D2/6-31G(d,p) molecular wavefunctions (see SI, Figure S4 and Table S3). The crystallographic information files (cifs) of Forms I and II were used for the calculations. The 2D plots were shaped by binning (di, de) pairs in the intervals of 0.01 Å and colouring each bin of the resulting 2D histogram as a function of the fraction of surface points in that bin, ranging from blue through green to red.

For energy frameworks calculations, the hydrogen atoms in the Forms I and II were normalized to standard neutron diffraction values. For each molecule in the asymmetric unit of a crystal, the total intermolecular interaction energy with another molecule, calculated using the B3LYP-D2/6-31G(d,p) electron densities model, is the sum of electrostatic, polarization, dispersion, and exchange-repulsion components with scaling factors of 1.057, 0.740, 0.871, and 0.618, respectively. The interaction energies of a selected molecule with all molecules having any atom within 3.8 Å were calculated. The interaction energies below certain energy threshold (5 kJ/mol) were omitted for clarity, and the cylinder thickness was taken to be proportional to the intermolecular interaction energies in the energy framework.

Attachment Energy and Elastic Constant Calculations. The attachment energy of indented crystal faces for CA-GA polymorphs were calculated with Forcite module in Materials Studio 6.0 using Drieding force field and charges Q_{eq} at ultra-fine quality (Table S4). The elastic constants for Forms I and II were calculated with Forcite module in Materials Studio 6.0 using Compass II force field and charges Q_{eq} at ultra-fine quality (Figure S5). The "Ewald" electrostatic summation method and "atom based" van der Waals summation were chosen for all calculations. The convergence thresholds during atomic coordinate geometry optimization were set at 10^{-5} Hartree (energy), 0.002 Hartree $Å^{-1}$ (max. force), and 0.005 Å (max. displacement), while the unit cell dimensions were fixed. A 6 × 6 symmetric elastic constants matrix were calculated to understand the stress−strain relationship for both forms. The bulk moduli, shear moduli, Young's moduli, and Poisson's ratio were calculated from the matrix based on the elasticity theory. The crystal anisotropy index was calculated as the ratio of the largest to the smallest Young's modulus.[65]

RESULTS AND DISCUSSION

The two polymorphs of CA-GA cocrystal (1:1) were obtained by liquid-assisted grinding and solution crystallization.[52] The morphologies of the CA−GA cocrystal polymorphs (Forms I and II) were distinctly different under the optical microscope, i.e., needle-shaped crystals for Form I and block-shaped crystals for Form II (see SI, Figure S2). In this study, the nanoindentation measurements have been performed at the room temperature therefore the

crystal structures of dimorphs determined at the room temperature are considered. Notably, the elusive unit cell differences have been reported for Form I at room temperature (RT) to that of the low temperature (180 K) suggest the possibility of a structural modulation in Form I between RT and low temperature crystal structures.[55] Herein we collected the full data and determined the crystal structure of Form I at RT for the first time, whose unit cell matched with a reported unit cell at the same conditions.[55] Form I at RT crystallizes in monoclinic system with $P2_1/m$ space group (CCDC number: **2011984**) whereas Form II at RT crystallizes in triclinic system with P-1 space group (Refcode: **EXUQUJ**) has been considered in this study. Both the forms contain 1:1 stoichiometry of caffeine and glutaric acid molecules in the asymmetric units (see SI, Table S1). The CA-GA dimorphs exhibit an identical secondary architecture and similar hydrogen-bond synthons such that a two-dimensional (2D) sheet forms from an array of linear O–H···O hydrogen bonds between the hydroxyl and the carbonyl groups of the glutaric acid molecules (Figure 1 and Table S2). Next, another carboxylic O–H group of glutaric acid is connected with the imidazole ring of caffeine via an O–H···N hydrogen bond and also the same carbonyl group of glutaric acid forms various weak C–H···O hydrogen bonds with caffeine. In Form II, the glutaric acid connects with caffeine through three different types of weak C–H···O hydrogen bonds whereas Form I consists of only two types of weak C–H···O hydrogen bonds (Figure 1). The flat 2D hydrogen-bonded sheets form layers. There is a marginal difference in the orientation of the molecules in particular owing to glutaric acid coformer within the layers of the two polymorphs. A conformational difference between the forms is due to the torsional rotation of the methylene carbons of glutaric acid as shown in the overlay Figure 2. Form I forms parallel tapes with the stacking arrangement of caffeine and glutaric acid molecules in an alternating fashion to connect through the weak C–H···O and C–H···π interactions, resulted into a flat layer. However, the slightly tilted tapes in Form II resulted in the corrugated layer formation and also the tapes are stacked via π···π interactions and parallelly connected through weak C–H···O and C–H···π interactions. It is also worth to note here that the packing difference between the two forms is also associated with a change in the conformation of the alkyl chain of the glutaric acid molecules (Figure 2).

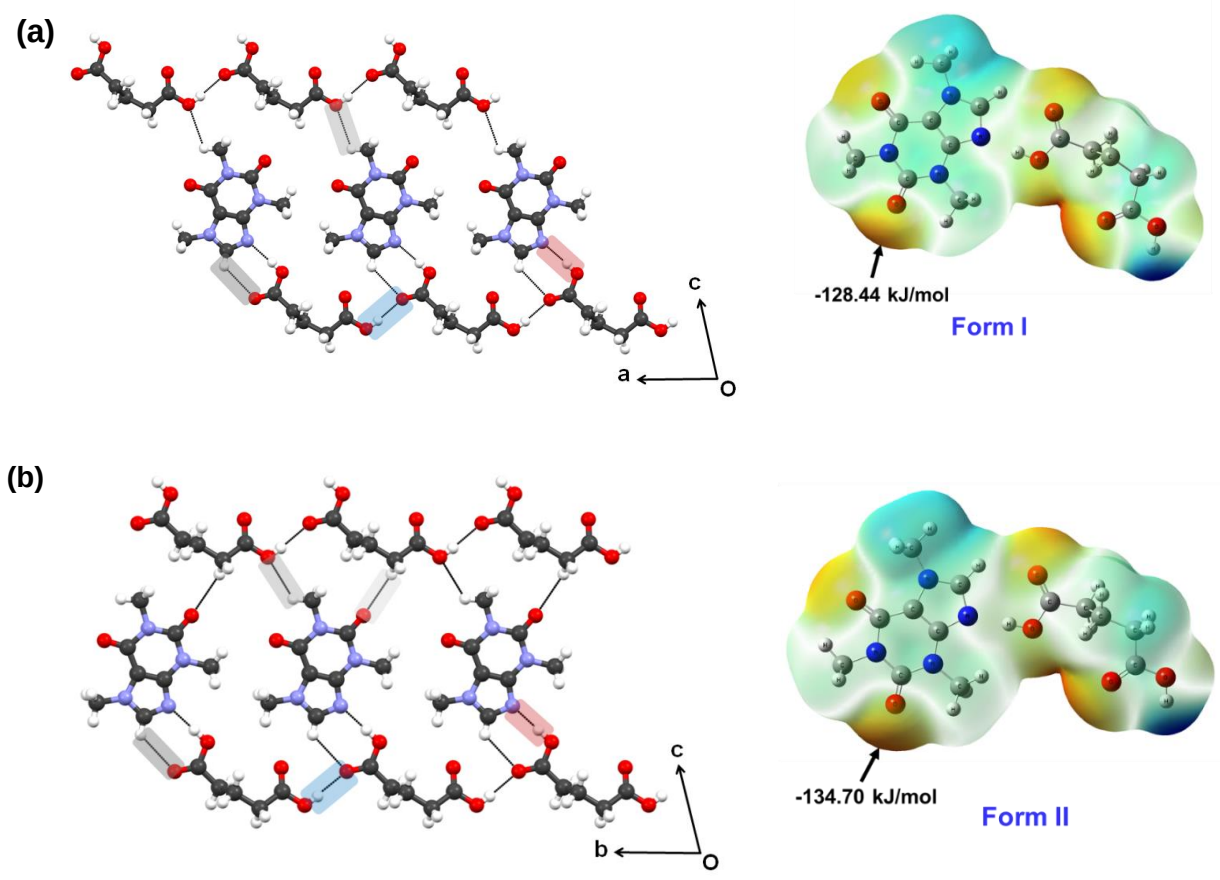

Figure 1. Hydrogen bond patterns and molecular electrostatic potential maps of Form I (a) and Form II (b) of CA–GA cocrystal polymorphs; color code: O–H···O (blue), O–H···N (red) and various C–H···O (grey).

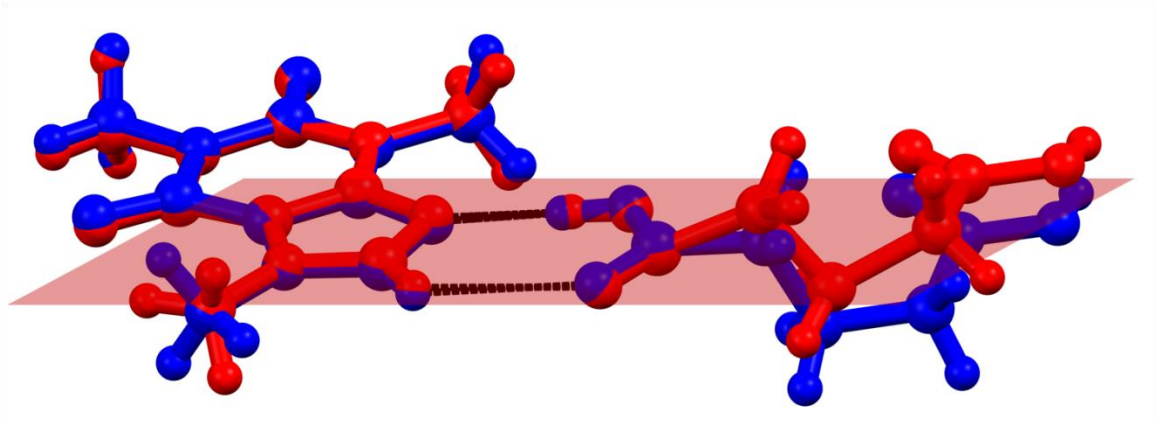

Figure 2. Structural overlay of caffeine and glutaric acid molecules in the Form I (red) and Form II (blue) of CA-GA cocrystal showing the conformational differences in the alkyl chain of the glutaric acid molecules.

Frontier molecular orbitals (FMOs) have been used to describe the chemical reactivity,[66] stability[66] and mechanical behavior[67-69] of molecular complexes by calculating their HOMO and LUMO energy gap (see SI, Figure S1). The HOMO-LUMO energy gap is inversely correlated with molecular polarizability[66] and the molecular polarizability is inversely correlated with mechanical properties such as E and H.[67-71] Therefore, a direct correlation between energy gap and mechanical property can be established.[69] When the energy gap is small, the molecule is highly polarizable, usually associated with low thermodynamic stability,[66] high chemical reactivity[66] and mechanical softness.[70,71] Computational results show that the energy gap of Form I (5.0956 ev) is less than Form II (5.1318 ev) thereby the Form II is expected to have high stability, lower chemical reactivity (higher physical stability) and high mechanical hardness than Form I.

In order to gain some molecular level information such as intermolecular interactions and variation in polarity, it has been performed the DFT analysis and calculated Molecular Electrostatic Potential (MEP) maps for both Forms I and II (Figure 1).[66] In general, as per MEP representation, the blue region is electropositive, the reddish region is electronegative, and the green region is neutral environment. In both the CA-GA dimorphs, the oxygen, O11 of the caffeine interacts with glutaric acid via weak C–H···O bonds. The negative electrostatic potential of O11 atom of Form II (-134.70 kJ/mol) is slightly higher than that of Form I (-128.44 kJ/mol). As a result, it is observed that O11 atom of Form II interacts with glutaric acid via numerous C–H···O interactions as compared to Form I.

Nanoindentation experiments were performed on the (001) and (100) faces of CA-GA dimorphs using the TI Premier Triboindenter (Hysitron, Minneapolis, MN) with an *in-situ* AFM imaging capability. Representative load, P, vs. depth of penetration, h, (P-h) curves of CA-GA cocrystal polymorphs are displayed in the Figure 3, which shows that the residual depth of penetration upon complete unloading, h_r, of both the faces of Form I is less than that of both the faces of Form II. Additionally, the AFM topographic indent images show no material pile-up along the edges of the indenter impressions on both faces of Form I, whereas small pile-up was

seen in Form II faces (See Figure S3). This implies that the resistance to plastic flow in Form I is less than that of Form II. *E* and *H* values with corresponding faces of the CA-GA cocrystal polymorphs extracted from *P-h* curves (Table 1) indicate that Form II is stiffer and harder than that of Form I.

Table 1. Elastic Modulus (*E*), Hardness (*H*), H/E Ratio, Indented Faces, and Slip Systems of CA-GA Cocrystal Polymorphs

Form	Abbreviation	Indented face	Hardness, *H* (MPa)	Elastic modulus, *E* (GPa)	*H/E*	Facile slip plane, Slip direction
Form I	$FI_{(001)}$	(001)	686.4 ± 5.8	18.02 ± 0.04	0.038	{010} <001>
	$FI_{(100)}$	(100)	330.1± 1.2	17.60± 0.49	0.019	{010} <100> and {001}<100>
Form II	$FII_{(001)}$	(001)	874.2 ± 2.7	19.35 ± 0.57	0.045	{101} <111>
	$FII_{(100)}$	(100)	960.0 ± 6.4	18.60 ± 0.35	0.051	{101} <111>

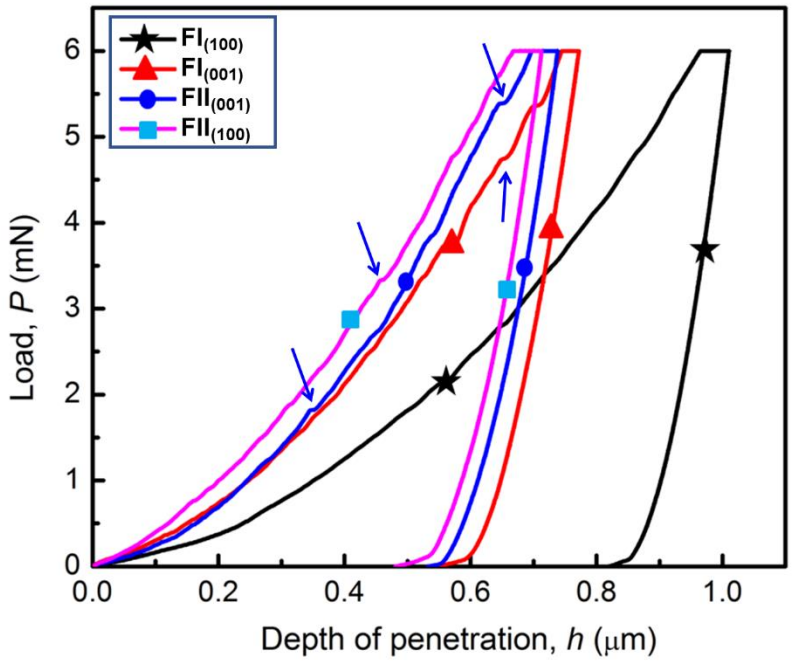

Figure 3. Representative *P–h* curves of the CA-GA cocrystal polymorphs. Blue arrows represent pop-ins.

It is important to understand the mechanical properties in the context of the molecular crystals. *E* depends upon the magnitude of the resistance offered by a material to elastic deformation.[15,16,21] It depends predominately on the nature of crystal packing, the strength of intermolecular interactions and their orientation with respect to the direction of indentation. Thus, the observed difference in *E* of the respective faces in these two forms of CA-GA cocrystal is due to the difference in the type, number and strength of intermolecular interactions and the difference in their orientation with respect to indentation direction. Interestingly, the *E* of the $FI_{(001)}$ and $FII_{(001)}$ were slightly higher than $FI_{(100)}$ and $FII_{(100)}$, respectively, due to lower inclination of the strong O–H···O and N–H···O and weak C–H···O hydrogen bonds with respect to the indentation direction. Overall, *E* of Form I was found to be lower than Form II. The number of C–H···O hydrogen bonds are relatively fewer between the layers of Form I, which favours an easy sliding of layers under applied load and therefore Form I is less elastic than Form II. Hirshfield surface analysis also shows that the percentage of O···H contacts of Form II which belongs to O–H···O, N–H···O and C–H···O hydrogen bonds is higher (~ 8%) than that of Form I (Figure 4 and see also SI, Figure S4). Therefore, the higher contribution of O···H contacts is consistent with the slightly higher *E* value of Form II with respect to Form I.

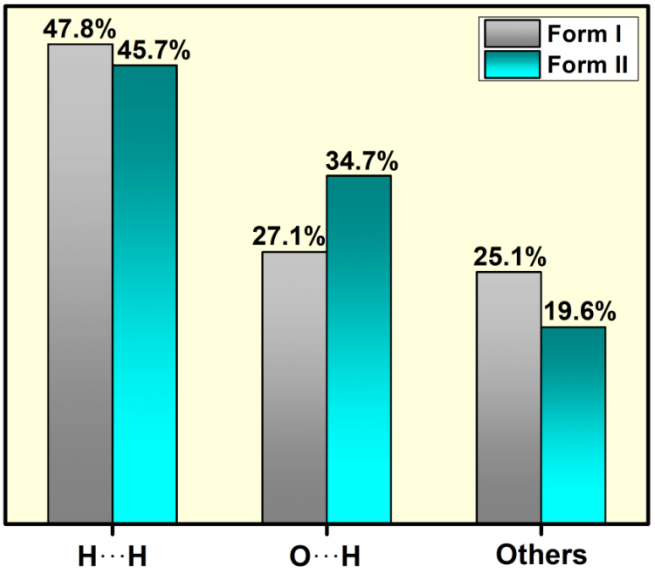

Figure 4: Hirshfield surface analysis of CA−GA cocrystal polymorphs. Note the O···H contacts for Form II is substantially higher (~8%) than that of Form I.

It is known that *H* is a measure of the resistance to plastic or permanent deformation of the indented material which depends on the relative ease of irrecoverable sliding of the molecular layers or slip planes on each other during the applied load.[15,16,21] Such slip typically takes place on specific slip systems, which are combinations of crystallographic planes with directions referred to as slip planes {*hkl*} and slip directions [*h'k'l'*], respectively. In general, slip planes associate with the least attachment energy, E_{att},[31] whereas the slip directions are those along which the shortest lattice translation is possible (Table S4). It is to be noted that many slip planes can theoretically be possible for any molecular crystals. However, all are not active or equally facile to allow slip in all conditions. Facile slip planes are those which exhibit the least interlayer and highest intralayer interaction energy, generally, with smooth slip layer topology. The slip systems were accurately identified for both the forms by structure visualization with focusing on the hydrogen bonding interactions and packing, attachment energy calculation and energy framework calculations (Table S3 and S4).[31] For CA-GA cocrystal forms, the first facile slip system for $FI_{(001)}$ and $FI_{(100)}$ are {010}<001>, and {010}<100> respectively, however, the facile slip system for both $FII_{(100)}$ and $FII_{(001)}$ is same, namely {101}<111>. The *P*−*h* responses recorded on the $FI_{(001)}$, $FII_{(100)}$ and $FII_{(001)}$ show pop-ins. The average values of $h_{pop\text{-}in}$ correspond to the integer multiples of interplanar *d* spacing, d_{hkl} of $FI_{(001)}$, $FII_{(100)}$, and $FII_{(001)}$ (Table S4). It can be noted that the second facile slip plane {001}<100> is also present in $FI_{(100)}$, however, absent in $FI_{(001)}$ (Figure 5a, b and c). The second facile slip plane in $FI_{(100)}$ provides excess ease to glide the layers on each other under applied load and consequently, $FI_{(100)}$ is substantially softer than $FI_{(001)}$. It can also be seen that the several pop-ins were observed on the loading curve of $FI_{(001)}$ whereas, no pop-ins were observed in case of $FI_{(100)}$ due to the availability of second facile slip plane. Interestingly, there is no second facile slip plane present in both $FII_{(001)}$ and $FII_{(100)}$. The orientation of the slip plane to the indentation direction (i.e., direction perpendicular to indented crystal face) is around 147° and 129° in $FII_{(001)}$ and $FII_{(100)}$, respectively (Figure 5d). These orientation differences suggest that the molecular layers of $FII_{(001)}$ can offer less resistance to shear sliding under applied load as compared to the $FII_{(100)}$ because of the higher oblique angle. Consequently, $FII_{(001)}$ is slightly softer than $FII_{(100)}$ due to the higher inclination angle (147°) between the molecular layers and indentation direction. These observations suggest that

Form I is more anisotropic than Form II in terms of hardness, however, both the forms are elastically isotropic. It is also worth to note here that overall Form II is harder than Form I, which could be rationalized by their structural differences. In Form I, the molecular layers are planar, however, in case of Form II, the layers are corrugated due to the twisted conformation of the glutaric acid that makes the gliding of layers past each other more difficult under the applied stress and therefore, Form II is hard vis-à-vis Form I. Furthermore, this lack of plastic deformability in Form II makes it stiffer compared to Form I.

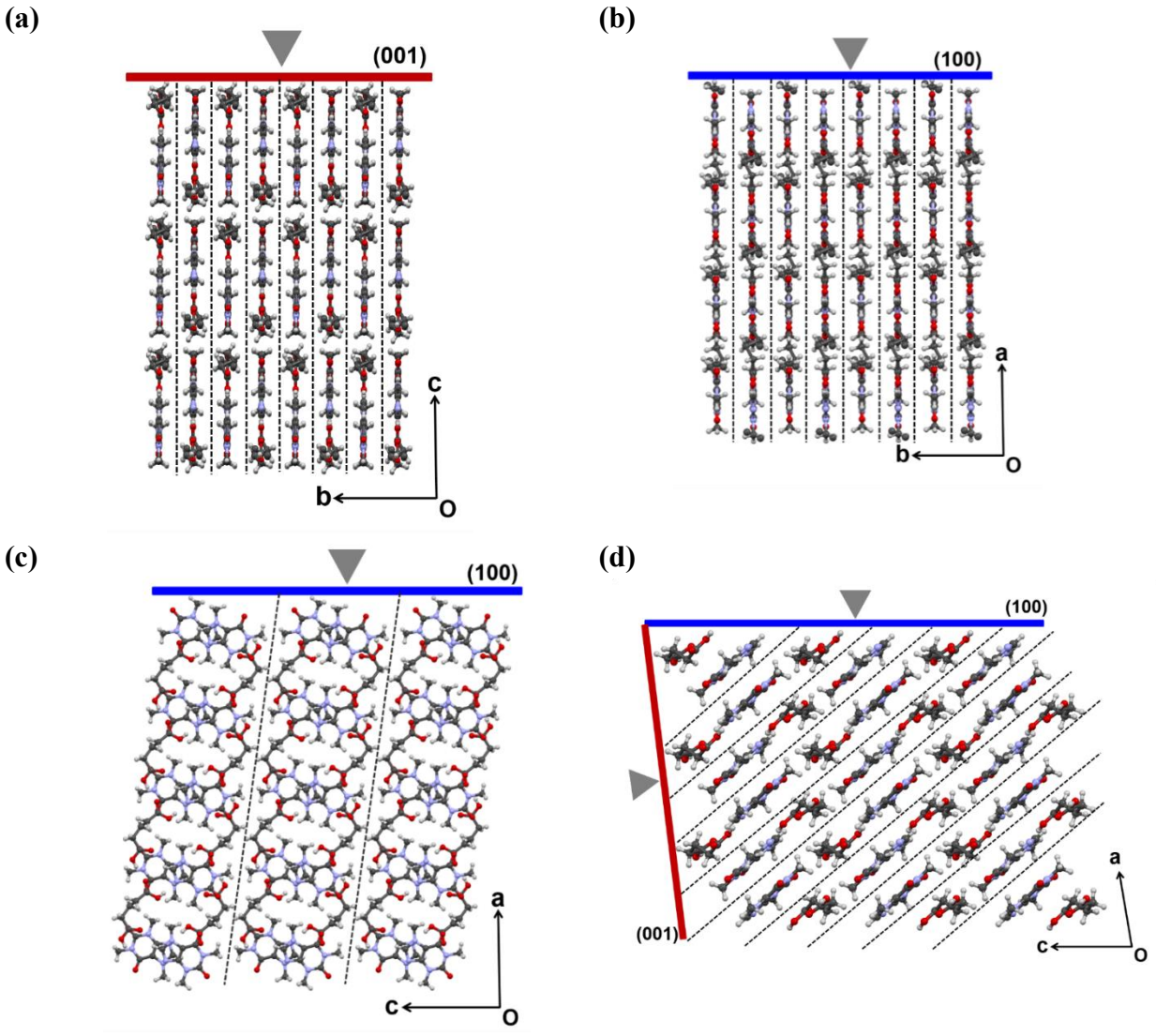

Figure 5. Molecular packing of (a) $FI_{(001)}$, (b) $FI_{(100)}$ with first facile slip plane, (c) $FI_{(100)}$ with second facile slip plane and (d) both $FII_{(100)}$ and $FII_{(001)}$ of CA-GA cocrystal polymorphs. Red and blue lines represent the plane (001) and (100) respectively, on which indentation is made.

The grey triangle represents the indentation direction and black dotted lines represent the possible slip planes of the polymorphs.

The energy framework calculations have been performed for visualising the topologies of interaction energies to provide insights into the structure-mechanical properties of the dimorphs of CA-GA cocrystal (Figure 6; see SI, Table S3).[50,72] The thickness of representative cylinders connecting the corresponding molecules are directly proportional to the strengths of pairwise intermolecular interactions between nearest neighbouring molecules. The distinct intermolecular interaction topologies of both CA-GA polymorphs are in good agreement with their distinct mechanical properties. The molecular layers are interconnected in both the polymorphs via π···π stacking and multiple C–H···O and C–H···π interactions. The interlayer energy in Form II (−129 kJ/mol) is substantially higher than Form I (−105 kJ/mol), which could be attributed to the presence of relatively significant parallel-displaced π–stacking interactions between caffeine molecules in Form II. The higher interlayer bonding energies affirmed the larger energetic barrier for sliding molecular layers along the potential slip plane during nanoindentation. Hence, Form I can undergo more facile deformation under load when compared to Form II. This clearly explains the lower *H* and *E* of Form I than Form II.

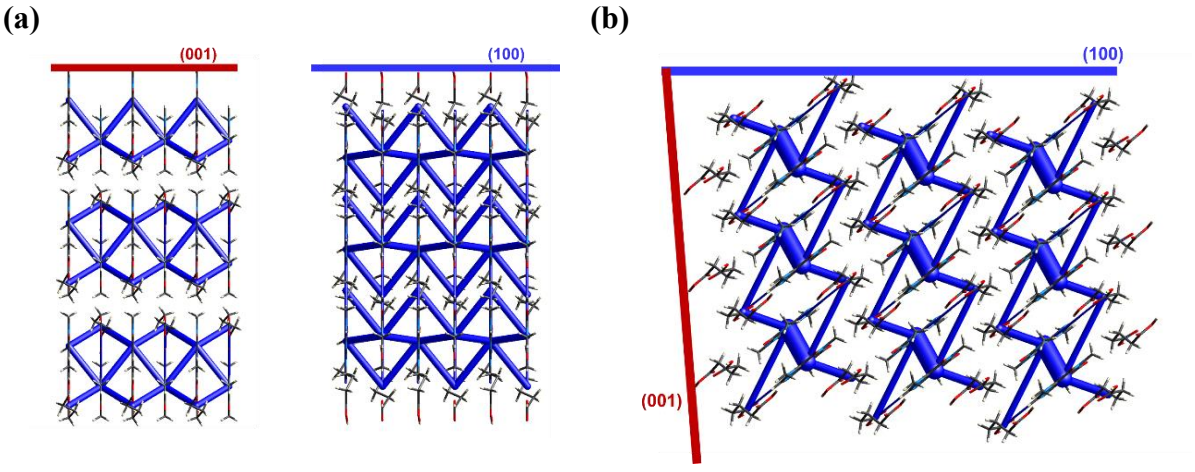

Figure 6. Energy frameworks analysis of (a) Form I and (b) Form II of CA-GA polymorphs. The thickness of each cylinder (in blue) represents the relative strength of pairwise intermolecular interactions. The energy threshold for the energy framework is set at − 5 kJ/mol. Red and blue bars represent the indentation planes.

To further explore the mechanical anisotropy, we have computed the elastic matrices of both polymorphs using Forcite module applying COMPASS II force field using QEq charges in Materials Studio (see Figure S5).[31] Such calculations have previously been utilized to rationalize the mechanical properties of polymorphic pharmaceutical drugs like paracetamol, aspirin and carbamazepine.[31] Three-dimensional distribution of E-map is represented in the SI, Figure S5. The higher bulk modulus of Form II (12.68 GPa) suggests its lower compressibility as compared to Form I (10.01 GPa). The computed anisotropy index of Form I (10.43) is relatively higher than that of Form II (8.32). This suggests that the Form I display higher mechanical anisotropy, leading to its higher plasticity as compared to Form II. These results are in excellent agreement with the experimental nanoindentation results, which obtained from different crystal faces of the dimorphs.

Thakuria *et al.* performed nanoindentation experiments on a single face (001) of both the polymorphs of CA−GA cocrystal to show the use of nanoindentation toward polymorphs discrimination.[56] However, the measuring of mechanical properties of a crystal in a single face is often inadequate for critical consideration such as crystalline drug choice in guiding pharmaceutically relevant processes like milling, flow, granulation and compaction.[44,45] Therefore, rationalizing the structure-mechanical properties correlations allied to the anisotropy in crystalline materials requires diligent attention for macroscopic pharmaceutical formulation and development process.[73,74] In this regard, our work on the measured anisotropic mechanical responses on multiple crystallographic faces of CA-GA cocrystal polymorphs would provide comprehensive information to predict the pharmaceutical formulation and performance in the early stage of drug development. Previously, it has been reported by us that Form II is thermodynamically stable, and Form I is metastable at ambient conditions based on thermal and slurry studies.[53] Here, our results suggest that the thermodynamically stable form, Form II is less plastic and more elastic than metastable form, Form I. It also shows that thermodynamically stable polymorph (Form II) is mechanically isotropic with high H and E, as compared to metastable form (Form I) which is more anisotropic with lower H and E values. Similar mechanical behaviors have also been observed in many polymorphic systems studied by us an others like curcumin, aspirin, felodipine, caffeine:4-chloro-3-nitrobenzoic acid cocrystals,

etc.[35,37,75] Tableting properties of the pharmaceutical drugs predominately depend upon the ability of its crystals to undergo plastic deformation under applied external load.[11,22] Two contrasting facts need to be considered to understand the mechanical performance of crystalline organic/pharmaceutical materials. First, the plasticity is absolutely crucial so as to increase the inter-particulate contact area and binding during compaction in other words for an improved tabletability. Second, if excessive plastic deformation takes place due to a very low *H*, one may end up with a pasty or gummy material that would be extremely difficult to mill. On the other hand, a brittle material would be suitable for milling process, however, it could suffer from lack of plastic deformation thus undesirable tabletability. Hence, a material with the optimal mechanical properties meaning plasticity is essential to achieve both millability and tabletability. Lawn and Marshall proposed that the brittleness index (BI) of a crystal, which is associated to the ratio of indentation hardness (*H*) to indentation fracture toughness (K_{IC}).[76] A material with higher value of BI (i.e., higher *H* and lower K_{IC}) can be considered as brittle, which promotes the fracturing of materials during milling process.[77] In general, a material with lower BI and higher K_{IC} can be envisaged to achieve the better tabletability and compaction properties.[78] Our results suggest that the Form I could display relatively better tabletability compared to that of Form II, which is in contrast to the order proposed by Thakuria *et al*.[56,79]

The resistance to plastic deformation can be estimated for a crystal by assessing *H* through nanoindentation, however, BI measurement may not always be possible. Generally, the K_{IC} of a material can only be measured if there are cracks during indentation.[76] In our case, the AFM images of indents show no cracks on the edges of the indenter impressions on both forms (See SI, Figure S3). Accordingly, the ratio of *H*/*E* can be considered in the absence of cracks.[19,77,78] Based on this approach, it has been demonstrated that a low *H*/*E* value shows better compaction behaviour for the APIs. The *H*/*E* values for the faces of both the polymorphs are provided in the Table 1. As seen, both faces, $FII_{(100)}$ and $FII_{(001)}$, of Form II with highest *H*/*E* ratio expect to display relatively poor compaction behavior compared to that of Form I.

Adherence of the solid powder on to tooling surface during tablet compaction, known as punch sticking, is one of the common tablet manufacturing obstacles.[80] Severe punch sticking significantly reduces the tablet quality. Many factors can affect punch sticking process such as crystal morphology, particle shape and size, excipients, surface energy and manufacturing

conditions.[80] It has been studied that a less plastic material reduces punch sticking propensity during compression by lowering powder-punch adhesion.[81] Hence, the less plastic Form II may show lower punch sticking during tablet formulation as compared to the Form I.

CONCLUSIONS

In conclusion, herein we systematically examined the mechanical anisotropy in the CA-GA cocrystal polymorphs, Forms I and II, on multiple faces of nanoindentation experiments under applied load. Higher hardness, *H*, and elastic modulus, *E*, of cocrystal Form II compared to that of metastable Form I has been observed. It is explained on the basis of its corrugated layers, higher interlayer energy, lower interlayer separation, and the presence of more intermolecular interactions in the crystal structure. The anisotropy and the plastic deformation in two polymorphs suggest that the difference in the structural features, namely possible slip systems, number and strength of the intermolecular interactions with respect to the indentation direction govern the variations in *E* and *H*. Overall, the results suggest that the CA-GA cocrystal Form I could display relatively better tabletability than that of Form II. Accordingly, an in-depth correlation of mechanical properties with the crystal structures may aid pharmaceutical crystal engineers to acquire improved formulation strategies in the early stage of drug development.

ASSOCIATED CONTENT

Supporting Information

The Supporting Information is available free of charge on the ACS Publications website at DOI: 10.1021/xxx.xxxxx. Intermolecular interaction energies, attachment energy calculation, crystallographic parameters, Hirshfeld surface images, HOMO-LUMO diagram, face indexing images, indented AFM images, and 3D-elastic constant diagrams of CA-GA polymorphs.

Accession Codes

CCDC 2011984 contains the supplementary crystallographic data for this paper. This data can be obtained free of charge via www.ccdc.cam.ac.uk/data_request/cif, or by emailing

data_request@ccdc.cam.ac.uk, or by contacting The Cambridge Crystallographic Data Centre, 12 Union Road, Cambridge CB2 1EZ, UK; fax: +44 1223 336033.

AUTHOR INFORMATION

Corresponding Authors:

*Venu R. Vangala: 0000-0002-0836-2052; Email: V.G.R.Vangala@bradford.ac.uk ; Phone: +441274236116

*C. Malla Reddy: 0000-0002-1247-7880; Email: cmreddy@iiserkol.ac.in

* Manish Kumar Mishra: 0000-0002-8193-3499; Email: mishra_mani07@yahoo.in

Authors

Kamini Mishra: 0000-0001-9514-9024

Aditya Narayan: 0000-0002-2301-0493

Complete contact information is available at: https://pubs.acs.org/10.1021/acs.cgd.xxxxxxx

Author Contributions

The manuscript was written through contributions of all authors. All authors have given approval to the final version of the manuscript.

Notes

The authors declare no competing financial interest.

Funding

V.V. and A. N. acknowledge the Government of India for National Overseas Scholarship and High Commission of India, London, UK for A.N.'s PhD studentship. CMR thanks DST, New Delhi for Swarnajayanti Fellowship (DST/SJF/CSA-02/2014-15) and SERB funding (No: EMR/2017/005008).

ACKNOWLEDGMENT

We profoundly thank Prof. Gautam R. Desiraju at the Indian Institute of Science, Bangalore, India for his inspiration and for stimulating this collaboration, which resulted in this publication work. We also thank Dr Jagadeesh Babu Nanubolu, CSIR-Indian Institute of Chemical Technology, Hyderabad, India for his knowledgeable support with the refinement of CA-GA Form I discussed in this study.

REFERENCES

1. Yousef, M. A. E.; Vangala, V. R. Pharmaceutical Cocrystals: Molecules, Crystals, Formulations, Medicines, *Cryst. Growth Des.* **2019**, *19*, 7420-7438.
2. Bolla, G.; Nangia, A. Pharmaceutical Cocrystals: Walking The Talk. *Chem. Commun*. **2016**, 52, 8342–8360.
3. Duggirala, N. K.; Perry, M. L.; Almarsson, Ö.; Zaworotko, M. J. Pharmaceutical Cocrystals: Along The Path To Improved Medicines. *Chem. Commun*. **2016**, *52*, 640–655.
4. Wang, G.; Hu, W.-B.; Zhao, X.-L.; Liu, Y. A.; Li, J.-S.; Jiang, B.; Wen, K. Engineering A Pillar [5] Arene-Based Supramolecular Organic Framework by A Co-Crystallization Method. *Dalton Trans*. **2018**, *47*, 5144–5148.
5. Aitipamula, S.; Vangala, V. R. X-Ray Crystallography and its Role in Understanding The Physicochemical Properties of Pharmaceutical Cocrystals, *J. Ind. Inst. Sci.* **2017**, *106*, 2009-2014.
6. Almarsson, Ö.; Zaworotko, M. J. Crystal Engineering of The Composition of Pharmaceutical Phases. Do Pharmaceutical Co-Crystals Represent A New Path to Improved Medicines? *Chem. Commun*. **2004**, 1889–1896.
7. Desiraju, G. R. Crystal Engineering: From Molecule to Crystal. *J. Am. Chem. Soc*. **2013**, *135*, 9952–9967.
8. McNamara, D. P.; Childs, S. L.; Giordano, J.; Iarriccio, A.; Cassidy, J.; Shet, M. S.; Mannion, R.; O'Donnell, E.; Park, A. Use af A Glutaric Acid Cocrystal To Improve Oral Bioavailability of A Low Solubility API. *Pharm. Res*. **2006**, *23*, 1888–1897.

9. Sanphui, P.; Tothadi, S.; Ganguly, S.; Desiraju, G. R. Salt And Cocrystals of Sildenafil With Dicarboxylic Acids: Solubility And Pharmacokinetic Advantage of The Glutarate Salt. *Mol. Pharmaceutics* **2013**, *10*, 4687-4697.
10. Jones, W.; Motherwell, W. D. S.; Trask, A. V. Pharmaceutical Cocrystals: An Emerging Approach To Physical Property Enhancement. *MRS Bull.* **2006**, *31*, 875–879.
11. Sun, C. C.; Hou, H. Improving Mechanical Properties of Caffeine And Methyl Gallate Crystals By Cocrystallization. *Cryst. Growth Des*. **2008**, *8*, 1575–1579.
12. Karki, S.; Friščič, T.; Fábián, L.; Laity, P. R.; Day, G. M.; Jones, W. Improving Mechanical Properties of Crystalline Solids By Cocrystal Formation: New Compressible Forms of Paracetamol. *Adv. Mater*. **2009**, *21*, 3905–3909.
13. Reddy, C. M.; Krishna, G. R.; Ghosh, S. Mechanical Properties of Molecular Crystals-Applications to Crystal Engineering. *CrystEngComm* **2010**, *12*, 2296-2314.
14. Kiran, M. S. R. N.; Varughese, S.; Reddy, C. M.; Ramamurty, U.; Desiraju, G. R. Mechanical Anisotropy in Crystalline Saccharin: Nanoindentation Studies. *Cryst. Growth Des*. **2010**, *10*, 4650–4655.
15. Varughese, S.; Kiran, M. S. R. N.; Ramamurty, U.; Desiraju, G., Nanoindentation in Crystal Engineering: Quantifying Mechanical Properties of Molecular Crystals. *Angew. Chem., Int. Ed.* **2013**, *52*, 2701-2712.
16. Saha, S.; Mishra, M. K.; Reddy, C. M.; Desiraju, G. R. From Molecules to Interactions to Crystal Engineering: Mechanical Properties of Organic Solids. *Acc. Chem. Res.* **2018**, *51*, 2957-2967.
17. Ghosh, S.; Reddy, C. M. Elastic and Bendable Caffeine Cocrystals: Implication For The Design of Flexible Organic Materials. *Angew. Chem., Int. Ed*. **2012**, *124*, 10465–10469.
18. Krishna, G. R.; Shi, L.; Bag, P. P.; Sun, C. C.; Reddy, C. M. Correlation Among Crystal Structure, Mechanical Behavior, And Tabletability In The Co-Crystals of Vanillin Isomers. *Cryst. Growth Des.* **2015**, *15*, 1827–1832.
19. Sanphui, P.; Mishra, M. K.; Ramamurty, U.; Desiraju, G. R. Tuning Mechanical Properties of Pharmaceutical Crystals with Multicomponent Crystals: Voriconazole as a Case Study. *Mol. Pharmaceutics* **2015**, *12*, 889–897.

20. Mondal, A,; Bhattacharya, B.; Das, S.; Bhunia, S.; Chowdhury, R.; Dey, S.; Reddy, C. M. Metal-like Ductility in Organic Plastic Crystals: Role of Molecular Shape and Dihydrogen Bonding Interactions in Aminoboranes. *Angew. Chem., Int. Ed*. **2020**, *132*, 11064-11073.
21. Mishra, M. K.; Ramamurty, U.; Desiraju, G. R. Mechanical Property Design of Molecular Solids. *Curr. Opin. Solid State Mater. Sci*. **2016**, *20(6)*, 361-370.
22. Sun, C. C. Materials Science Tetrahedron—A Useful Tool for Pharmaceutical Research and Development. *J. Pharm. Sci*. **2009**, *98*, 1671-1687.
23. Krishna, G. R.; Devarapalli, R.; Lal, G.; Reddy, C. M. Mechanically Flexible Organic Crystals Achieved by Introducing Weak Interactions in Structure: Supramolecular Shape Synthons. *J. Am. Chem. Soc.* **2016**, *138*, 13561–13567.
24. John, G.; Jadhav, S. R.; Menon, V. M.; John, V. T. Flexible Optics: Recent Developments in Molecular Gels. *Angew. Chem., Int. Ed.* **2012**, *51*, 1760–1762.
25. Cianchetti, M.; Laschi, C.; Menciassi, A.; Dario, P. Biomedical Applications of Soft Robotics. *Nat. Rev. Mater.* **2018**, *3*, 143–153,
26. Fratzl, P.; Barth, F. G. Biomaterial Systems for Mechanosensing and Actuation. *Nature* **2009**, *462*, 442– 448.
27. Lv, S.; Dudek, D. M.; Cao, Y.; Balamurali, M. M.; Gosline, J.; Li, H. Designed Biomaterials to Mimic the Mechanical Properties of Muscles. *Nature* **2010**, *465*, 69–73.
28. Cao, Y.; Li, H. Engineered Elastomeric Proteins with Dual Elasticity Can Be Controlled by A Molecular Regulator. *Nat. Nanotechnol.* **2008**, *3*, 512–516.
29. Manimunda, P.; Hintsala, E.; Asif, S.; Mishra, M. K. Mechanical Anisotropy and Pressure Induced Structural Changes in Piroxicam Crystals Probed by In Situ Indentation and Raman Spectroscopy. *JOM* **2017**, *69*, 57.
30. Manimunda, P.; Asif, S. A. S.; Mishra, M. K. Probing Stress Induced Phase Transformation in Aspirin Polymorphs Using Raman Spectroscopy Enabled Nanoindentation. *Chem. Commun.* **2019**, *55*, 9200–9203.
31. Wang, C.; Sun, C. C. Computational Techniques for Predicting Mechanical Properties of Organic Crystals: A Systematic Evaluation. *Mol. Pharmaceutics* **2019**, *16*, 1732-1741.
32. Wang, K.; Mishra, M. K.; Sun, C. C. Exceptionally Elastic Single-Component Pharmaceutical Crystals. *Chem. Mater.* **2019**, *31*, 1794-1799.

33. Hu, S.; Mishra, M. K.; Sun, C. C. Twistable Pharmaceutical Crystal Exhibiting Exceptional Plasticity and Tabletability. *Chem. Mater.* **2019**, *31*, 3818-3822.
34. Sun, C. C. Decoding Powder Tabletability: Roles of Particle Adhesion and Plasticity. *J. Adhes. Sci. Technol.* **2011**, *25*, 483–499.
35. Varughese, S.; Kiran, M. S. R. N.; Solanko, K. A.; Bond, A. D.; Ramamurty, U.; Desiraju, G. R. Interaction Anisotropy and Shear Instability of Aspirin Polymorphs Established by Nanoindentation. *Chem. Sci.* **2011**, *2*, 2236–2242.
36. Shakhtshneider, T. P.; Boldyrev, V. V. In *Reactivity of Molecular Solids*, ed. Boldyreva, E. V.; Boldyrev, V. V.Wiley, New York, 1999, p. 271.
37. Mishra, M. K.; Desiraju, G. R.; Ramamurty, U.; Bond, A. D. Studying Microstructure in Molecular Crystals with Nanoindentation: Intergrowth Polymorphism in Felodipine. *Angew. Chem., Int. Ed.* **2014**, *53*, 13102-13105.
38. Liu, F.; Hooks, D. E.; Li, N.; Mara, N. A.; Swift, J. A. Mechanical Properties of Anhydrous and Hydrated Uric Acid Crystals. *Chem. Mater*. **2018**, *30*, 3798–3805,
39. Mondal, P. K.; Bhandary, S.; Javoor, M. G.; Cleetus, A.; Kiran, M. S. R. N.; Ramamurty, U.; Chopra, D. Probing The Distinct Nanomechanical Behaviour of A New Co-Crystal and A Known Solvate of 5-Fluoroisatin and Identification of A New Polymorph. *CrystEngComm* **2020**, *22*, 2566-2572.
40. Devarapalli, R.; Kadambi, S. B.; Chen, C.-T.; Krishna, G. R.; Kammari, B. R.; Buehler, M. J.; Ramamurty, U.; Reddy, C. M. Remarkably Distinct Mechanical Flexibility in Three Structurally Similar Semiconducting Organic Crystals Studied by Nanoindentation and Molecular Dynamics. *Chem. Mater*. **2019**, *31*, 1391–1402.
41. Kiran, M. S. R. N.; Varughese, S.; Ramamurty, U.; Desiraju, G. R. Effect of dehydration on the mechanical properties of sodium saccharin dihydrate probed with nanoindentation. *CrystEngComm*, **2012**,*14*, 2489-2493.
42. SeethaLekshmi, S.; Kiran, M. S. R. N.; Ramamurty, U.; Varughese, S. Phase Transitions and Anisotropic Mechanical Response in a Water-rich Trisaccharide Crystal. *Cryst. Growth Des*. **2020**, *20*, 1, 442–448.
43. Krishna, G. R.; Kiran, M. S. R. N.; Fraser, C. L.; Ramamurty, U.; Reddy, C. M. The Relationship of Solid-State Plasticity to Mechanochromic Luminescence in Difluoroboron Avobenzone Polymorphs. *Adv. Funct. Mater*. **2013**, *23*, 1422–1430.

44. Hadjittofis, E.; Isbell, M. A.; Karde, V.; Varghese, S.; Ghoroi, C.; Heng, J. Y. Y. Influences of Crystal Anisotropy in Pharmaceutical Process Development. *Pharm. Res*. **2018**, *35*, 100.
45. Jaina, A.; Shahc, H. S.; Johnsona, P. R.; Narangd, A. S.; Morrise, K. R.; Hawarea, R. V. Crystal Anisotropy Explains Structure-Mechanics Impact on Tableting Performance of Flufenamic Acid Polymorphs. *Eur. J. Pharm. Biopharm*. **2018**, *132*, 83–92.
46. Mohamed, R. M.; Mishra, M. K.; Al-Harbi, L. M.; Al-Ghamdi, M. S.; Ramamurty, U. Anisotropy in The Mechanical Properties of Organic Crystals: Temperature Dependence. *RSC Adv*. **2015**, *5*, 64156–64162.
47. Mishra, M. K.; Sanphui, P.; Ramamurty, U.; Desiraju, G. R. Solubility-Hardness Correlation in Molecular Crystals: Curcumin and Sulfathiazole Polymorphs. *Cryst. Growth Des*. **2014**, *14*, 3054-3061.
48. Mishra, M. K.; Ramamurty, U.; Desiraju, G. R., Solid Solution Hardening of Molecular Crystals: Tautomeric Polymorphs of Omeprazole. *J. Am. Chem. Soc*. **2015**, *137*, 1794-1797.
49. Reddy, C. M.; Basavoju, S.; Desiraju, G. R. Sorting of Polymorphs Based on Mechanical Properties. Trimorphs of 6-chloro-2,4-dinitroaniline. *Chem. Comm.*, **2005**, 2439-2441.
50. Raju, K. B., Ranjan, S.; Vishnu, V. S.; Bhattacharya, M.; Bhattacharya, B.; Mukhopadhyay, A. K.; Reddy, C. M. Rationalizing Distinct Mechanical Properties of Three Polymorphs of a Drug Adduct by Nanoindentation and Energy Frameworks Analysis: Role of Slip Layer Topology and Weak Interactions. *Cryst. Growth Des*. **2018**, *18*, 3927-3937.
51. Velaga, S.; Vangala, V. R.; Srinivas, B.; Boström, D. Polymorphism in Acesulfame Sweetener: Structure–Property And Stability Relationships of Bending And Brittle Crystals. *Chem. Commun.* **2010**, *46*, 3562-3564.
52. Trask, A. V.; Motherwell, W. D. S.; Jones, W. Solvent-Drop Grinding: Green Polymorph Control of Cocrystallisation. *Chem. Commun*. **2004**, 890−891.
53. Vangala, V. R.; Chow, P. S.; Schreyer, M.; Lau, G.; Tan, R. B. H. Thermal And in Situ X-Ray Diffraction Analysis of A Dimorphic Co-Crystal, 1:1 Caffeine-Glutaric Acid. *Cryst. Growth Des.* **2016**, *16*, 578-586.
54. Chow, P. S.; Lau, G.; Ng. W. G.; Vangala, V. R. Stability of Pharmaceutical Cocrystal During Milling: A Case Study of 1:1 Caffeine-Glutaric Acid. *Cryst. Growth Des*. **2017**, *17*, 4064-4071.

55. Thakuria, R.; Eddleston, M. D.; Chow, E. H. H.; Lloyd, G. O.; Aldous, B. J.; Krzyzaniak, J. F.; Bond, A. D.; Jones, W. Use of In Situ Atomic Force Microscopy To Follow Phase Changes At Crystal Surfaces In Real Time. *Angew. Chem., Int. Ed*. **2013**, 52, 10541−10544.
56. Thakuria, R.; Eddleston, M. D.; Chow, E. H. H.; Lloyd, G. O.; Aldous, B. J.; Krzyzaniak, J. F.; Bond, A. D.; Jones, W. Comparison of Surface Techniques for The Discrimination of Polymorphs. *CrystEngComm* **2016**,*18*, 5296-5301.
57. RigakuMercury375R/M CCD, CrystalClear-SM Expert 2.0 rc14; Rigaku Corporation: Tokyo, Japan, 2009.
58. Sheldrick, G. M. A short history of SHELX *Acta Crystallogr.*, **2008**, *A64*, 112–122.
59. Farrugia, L. J. WinGX suite for small-molecule single-crystal crystallography. *J. Appl. Crystallogr*., **1999**, *32*, 837–838.
60. Frisch, M. J.; Trucks, G. W.; Schlegel, H. B.; Scuseria, G. E.; Robb, M. A.; Cheeseman, J. R.; Scalmani, G.; Barone, V.; Mennucci, B.; Petersson, G. A.; Nakatsuji, H.; Caricato, M.; Li, X.; Hratchian, H. P.; Izmaylov, A. F.; Bloino, J.; Zheng, G.; Sonnenberg, J. L.; Hada, M.; Ehara, M.; Toyota, K.; Fukuda, R.; Hasegawa, J.; Ishida, M.; Nakajima, T.; Honda , Y.; Kitao, O.; Nakai, H.; Vreven, T.; Jr. Montgomery, J. A.; Peralta, J. E.; Ogliaro, F.; Bearpark, M.; Heyd, J. J.; Brothers, E.; Kudin, K. N.; Staroverov, V. N.; Kobayashi, R.; Normand, J.; Raghavachari, K.; Rendell, A.; Burant, J. C.; Iyengar, S. S.; Tomasi, J.; Cossi, M.; Rega, N.; Millam, J. M.; Klene, M.; Knox, J. E.; Cross, J. B.; Bakken, V.; Adamo, C.; Jaramillo, J.; Gomperts, R.; Stratmann, R. E.; Yazyev, O.; Austin, A. J.; Cammi, R.; Pomelli, C.; Ochterski, J. W.; Martin, R. L.; Morokuma, K.; Zakrzewski, V. G.; Voth, G. A.; Salvador, P.; Dannenberg, J. J.; Dapprich, S.; Daniels, A. D.; Farkas, O.; Foresman, J. B.; Ortiz, J. V.; Cioslowski, J.; Fox, D. J. Gaussian 09, Revision E.01; Gaussian, Inc.: Wallingford, CT, 2009.
61. Gabriele, B. P.A.; Williams, C. J.; Lauer, M. E.; Derby, B.; Cruz-Cabeza, A. J. Nanoindentation of Molecular Crystals: Lessons Learnt from Aspirin. *Cryst. Growth Des*. **2020**, DOI: 10.1021/acs.cgd.0c00635.
62. Oliver, W. C.; Pharr, G. M., An Improved Technique for Determining Hardness and Elastic Modulus Using Load and Displacement Sensing Indentation Experiments. *J. Mater. Res*. **2011**, *7*, 1564-1583.

63. Bolshakov A.; Pharr G. M. Influences of pileup on the measurement of mechanical properties by load and depth sensing instruments. *J. Mater. Res*. **1998**, *13*, 1049-1058.
64. Turner, M. J.; McKinnon, J. J.; Wolff, S. K.; Grimwood, D. J.; Spackman, P. R.; Jayatilaka, D.; Spackman, M. A. CrystalExplorer17. http://hirshfeldsurface.net.
65. Ranganathan, S. I.; Ostoja-Starzewski, M. Universal elastic anisotropy index. *Phys. Rev. Lett*. **2008**, *101*, 055504.
66. Khan, E.; Shukla, A.; Srivastava, K., Gangopadhyay, D.; Assi, K. H.; Tandon, P.; Vangala, V. R. Structural and Reactivity Analyses of Nitrofurantoin–4-dimethylaminopyridine Salt Using Spectroscopic and Density Functional Theory Calculations. *Crystals* **2019**, *9*, 413.
67. Yang, W.; Parr, R. G.; Uytterhoeven, L. New Relation between Hardness and Compressibility of Minerals. *Phys. Chem. Miner.* **1987**, *15*, 191-195.
68. Gilman, J. J. Chemistry and Physics of Mechanical Hardness, 3rd ed.; Wiley: New York, 2009
69. Gilman, J. J. Chemical and Physical "Hardness". *Mater. Res. Innovations* **1997**, *1*, 71-76.
70. Donald, K. J. Electronic Compressibility and Polarizability: Origins of a Correlation. *J. Phys. Chem. A* **2006**, *110*, *6*, 2283–2289.
71. Rupasinghe, T. P.; Hutchins, K. M.; Bandaranayake, B. S.; Ghorai, S.; Karunatilake, C.; Bučar, D.-K.; Swenson, D. C.; Arnold, M. A.; MacGillivray, L. R.; Tivanski, A. V. Mechanical Properties of a Series of Macro- and Nanodimensional Organic Cocrystals Correlate with Atomic Polarizability. *J. Am. Chem. Soc*. **2015**, *137*, *40*, 12768–12771.
72. Turner, M. J.; Thomas, S. P.; Shi, M. W.; Jayatilaka, D.; Spackman, M. A. Energy Frameworks: Insights into Interaction Anisotropy and The Mechanical Properties of Molecular Crystals. *Chem. Commun*. **2015**, *51*, 3735-3738.
73. Wang, C. G.; Paul, S.; Wang, K. L.; Hu, S. Y.; Sun, C. C. Relationships among Crystal Structures, Mechanical Properties, and Tableting Performance Probed Using Four Salts of Diphenhydramine. *Cryst. Growth Des*. **2017**, *17*, 6030–6040;
74. Yadav, J. A.; Khomane, K. S.; Modi, S. R.; Ugale, B.; Yadav, R. N.; Nagaraja, C. M.; Kumar, N.; Bansal, A. K. Correlating Single Crystal Structure, Nanomechanical, and Bulk Compaction Behavior of Febuxostat Polymorphs. *Mol. Pharmaceutics* **2017**, *14*, 866–87.
75. Ghosh, S.; Mondal, A.; Kiran, M. S. R. N.; Ramamurty, U.; Reddy, C. M. The Role of Weak Interactions in the Phase Transition and Distinct Mechanical Behavior of Two Structurally

Similar Caffeine Co-crystal Polymorphs Studied by Nanoindentation. *Cryst. Growth Des*. **2013**, *13*, 4435–4441.

76. Lawn, B. R.; Marshall, D. B. Hardness, Toughness, and Brittleness: An Indentation Analysis. *J. Am. Ceram. Soc*. **1979**, *62*, 347–350.
77. Taylor, L. J.; Papadopoulos, D. G.; Dunn, P. J.; Bentham, A. C.; Dawson, N. J.;Mitchell, J. C.; Snowden, M. J. Predictive Milling of Pharmaceutical Materials Using Nanoindentation of Single Crystals. *Org. Process Res. Dev*. **2004**, *8*, 674–679.
78. Egart, M.; Janković, B.; Srčič, S. Application of Instrumented Nanoindentation In Preformulation Studies of Pharmaceutical Active Ingredients And Excipients. *Acta. Pharm.* **2016**, *66*, 303–330.
79. In the report of Thakuria et al.,[56] the measurement of K_{Ic} and BI for the two polymorphs of CA-GA could have suffered due to the inconsistent or poorly visible cracks in their indentation experiments.
80. Paul, S.; Taylor, L. J.; Murphy, B.; Krzyzaniak, J.; Dawson, N.; Mullarney, M. P.; Meenan, P.; Sun, C. C., Mechanism and Kinetics of Punch Sticking of Pharmaceuticals. *J. Pharm. Sci*. **2017**, *106*, 151-158.
81. Wang, C.; Paul, S.; Sun, D. J.; Lill, S. O. N.; Sun, C. C. Mitigating Punch Sticking Propensity of Celecoxib by Cocrystallization–An Integrated Computational And Experimental Approach. *Cryst. Growth Des*., **2020**, *20*, 4217-4223.

Table of Contents Graphic

Structural Basis for Mechanical Anisotropy in Polymorphs of Caffeine-Glutaric Acid Cocrystal

Manish Kumar Mishra,[a] Kamini Mishra,[b] Aditya Narayan,[c] C. Malla Reddy*[d] and Venu R. Vangala*[c]*

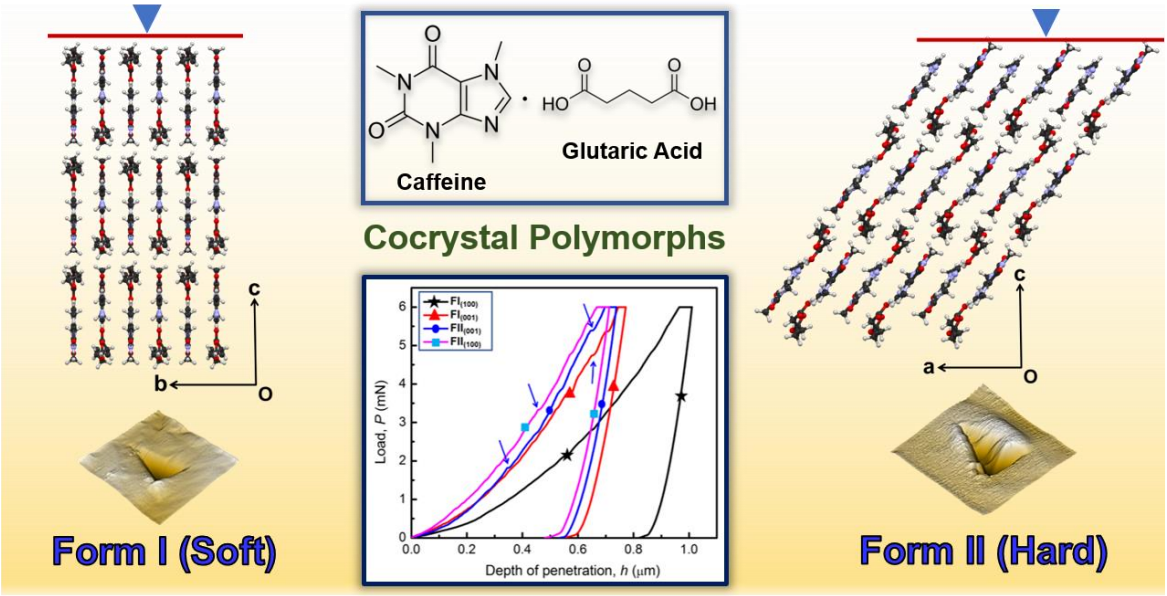

Insights into crystal structure and mechanical property correlations in dimorphic forms, Forms I and II, of 1:1 caffeine-glutaric acid cocrystal on multiple faces using nanoindentation suggest that metastable form (Form I) with higher plasticity could display suitable tablet performance over stable form, Form II. It demonstrates that multiple faces of nanoindentation is critical in determining mechanical anisotropy and in turn structure-mechanical property correlation.